

## Synthesis and Cytotoxicity of Water-Soluble Dual- and Triple-Action Satraplatin Derivatives: Replacement of Equatorial Chlorides of Satraplatin by Acetates

Subhendu Karmakar,<sup>†,||</sup> Isabella Poetsch,<sup>‡,§,||</sup> Christian R. Kowol,<sup>§,||</sup> Petra Heffeter,<sup>\*,‡</sup> and Dan Gibson<sup>\*,†,||</sup>

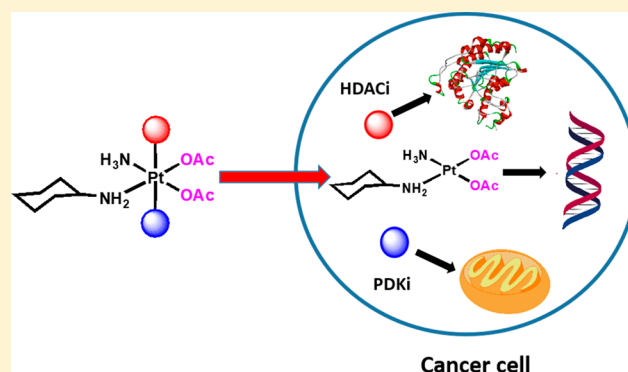
<sup>†</sup>Institute for Drug Research, School of Pharmacy, The Hebrew University, Jerusalem 91120, Israel

<sup>‡</sup>Institute of Cancer Research and Comprehensive Cancer Center, Department of Medicine I, Medical University of Vienna, Borschkegasse 8a, 1090 Vienna, Austria

<sup>§</sup>Institute of Inorganic Chemistry, Faculty of Chemistry, University of Vienna, Vienna, Austria

### Supporting Information

**ABSTRACT:** Pt(II) complexes, such as cisplatin and oxaliplatin, are in widespread use as anticancer drugs. Their use is limited by the toxic side effects and the ability of tumors to develop resistance to the drugs. A popular approach to overcome these drawbacks is to use their kinetically inert octahedral Pt(IV) derivatives that act as prodrugs. The most successful Pt(IV) complex in clinical trials to date is satraplatin, *cis*-[Pt(NH<sub>3</sub>)(c-hexylamine)Cl<sub>2</sub>(OAc)<sub>2</sub>], that upon cellular reduction releases the cytotoxic *cis*-[Pt(NH<sub>3</sub>)(c-hexylamine)Cl<sub>2</sub>]. In an attempt to obtain water-soluble and more effective cytotoxic Pt(IV) complexes, we prepared a series of dual- and triple-action satraplatin analogues, where the equatorial chlorido ligands were replaced with acetates and the axial ligands include innocent and bioactive ligands. Replacement of the chlorides with acetates enhanced the water solubility of the compounds and, with one exception, all of the compounds were very stable in buffer. In general, compounds with one or two axial hydroxido ligands were reduced by ascorbate significantly more quickly than compounds with two axial carboxylates. While replacement of the chlorides with acetates in satraplatin led to a reduction in cytotoxicity, the dual- and triple-action analogues with equatorial acetates had low- to sub-micromolar IC<sub>50</sub> values in a panel of eight cancer cells. The triple-action compound *cis*-[Pt(NH<sub>3</sub>)(c-hexylamine)(OAc)<sub>2</sub>(PhB)(DCA)] was active in all cell lines, causing DNA damage that induced cell cycle inhibition and apoptosis. Its good activity against CT26 cells in vitro translated into good in vivo efficacy against the CT26 allograft, an in vivo model with intrinsic satraplatin resistance. This indicates that multi-action Pt(IV) derivatives of diamine dicarboxylates are interesting anticancer drug candidates.



## INTRODUCTION

Platinum (Pt)-based cancer chemotherapy became immensely popular in the last four decades after its accidental discovery by Rosenberg et al.<sup>1–3</sup> The three FDA-approved Pt(II) drugs cisplatin, carboplatin, and oxaliplatin (Figure 1) are still helping cancer patients worldwide in the fight against this disease.<sup>4–7</sup> However, some serious side effects<sup>8–10</sup> and inherent and acquired drug resistances<sup>11–14</sup> prompted inorganic medicinal chemists to design better platinum-based drugs. Cisplatin, *cis*-[Pt(NH<sub>3</sub>)<sub>2</sub>Cl<sub>2</sub>], triggers its cytotoxic effect by losing its chlorido ligands and binding to two adjacent guanines on the same strand of the nuclear DNA. The drug is administered intravenously and enters the cancer cell by passive diffusion and through the human copper transporter (hCTR).<sup>15</sup> Outside the cell, it stays in the dichlorido form due to the high extracellular chloride concentration (~100 mM). Inside the cell, the chloride concentration is lower (4–10

mM), resulting in the activation of cisplatin by aquation, where *cis*-[Pt(NH<sub>3</sub>)<sub>2</sub>Cl<sub>2</sub>] is converted to the reactive *cis*-[Pt(NH<sub>3</sub>)<sub>2</sub>(H<sub>2</sub>O)Cl]<sup>+</sup>, which covalently modifies the DNA (Scheme 1). Thus, cisplatin itself can be considered a prodrug where a main role of the chlorido ligands is to stabilize the drug outside the cell and allow its activation inside.

Nowadays one of the most popular approaches to overcome these drawbacks is to use kinetically inert octahedral Pt(IV) derivatives of the semilabile square-planar cisplatin.<sup>16–18</sup> Pt(IV) complexes are derived from Pt(II) by oxidative addition, where two ligands are added to the axial positions. Their kinetic inertness minimizes unwanted extracellular interactions, but once inside the cancer cell the complex is

Received: September 19, 2019

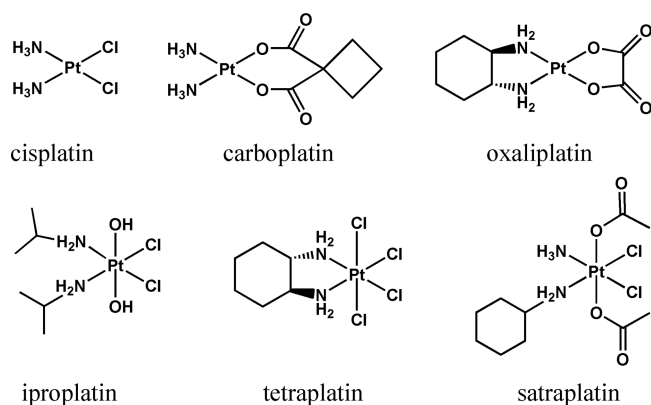


**Figure 1.** Three FDA-approved Pt(II) drugs (cisplatin, carboplatin, and oxaliplatin) and the three Pt(IV) complexes (iproplatin, tetraplatin/ormaplatin, and satraplatin) that have entered clinical trials.

reduced, releasing the original Pt(II) drug as well as the two axial ligands (Scheme 1).

Among the three Pt(IV) drugs (iproplatin, tetraplatin, satraplatin, Figure 1) that have entered clinical trials, satraplatin has shown encouraging activity in combination therapy and as a standalone drug.<sup>19–23</sup>

Pt(IV) compounds need to be activated inside the cell to release the Pt(II) drug that itself requires further activation. Since in this case, the Pt(II) drug is generated inside the cancer cell, it no longer requires the chlorido ligands for extracellular stabilization. Therefore, in principle, a Pt(II) drug with any labile or semilabile leaving group, which is generated inside the cancer cell, could be active as well. Thus, we decided to explore the Pt(IV) derivatives of satraplatin where the chlorido ligands were replaced by acetato groups. On the one hand, acetates bind to the Pt through the oxygen, making them good leaving groups, and on the other hand, they can increase the water solubility of the complexes.

Recently, it has become very popular to conjugate bioactive ligands to the axial positions of Pt(IV) complexes to attain “dual action” or “triple action” drugs.<sup>24–32</sup> On the basis of our previous experience, we decided to use histone deacetylase (HDAC) and/or pyruvate dehydrogenase kinase (PDK) inhibitors such as 4-phenylbutyrate (PhB) and/or dichloro-

oacetate (DCA), respectively, as the bioactive ligands. HDAC inhibitors play a pivotal role in the alteration of epigenetic mechanisms by changing the structure of chromatin, thereby controlling gene expression or repression.<sup>33–35</sup> Hence, HDAC inhibitors can act as drugs in epigenetic anticancer therapy. FDA has already approved the HDAC inhibitors SAHA (vorinostat),<sup>34,36</sup> belinostat,<sup>37</sup> and romidepsin<sup>38</sup> for the treatment of T-cell lymphoma and panabiostat<sup>39,40</sup> for multiple myeloma. The inhibition of PDK by DCA leads to activation of the pyruvate dehydrogenase complex (PDHC), resulting in a shift of cellular metabolism from glycolysis to glucose oxidation, which affects the survival of cancer cells.<sup>41,42</sup> DCA is considered an orphan drug, and its anticancer activity is well-known.<sup>43–45</sup>

Recently, Hoefler et al. showed that lipophilic Pt(IV) complexes with four monodentatecarboxylato ligands have good aqueous solubility and good cytotoxicity.<sup>46</sup>

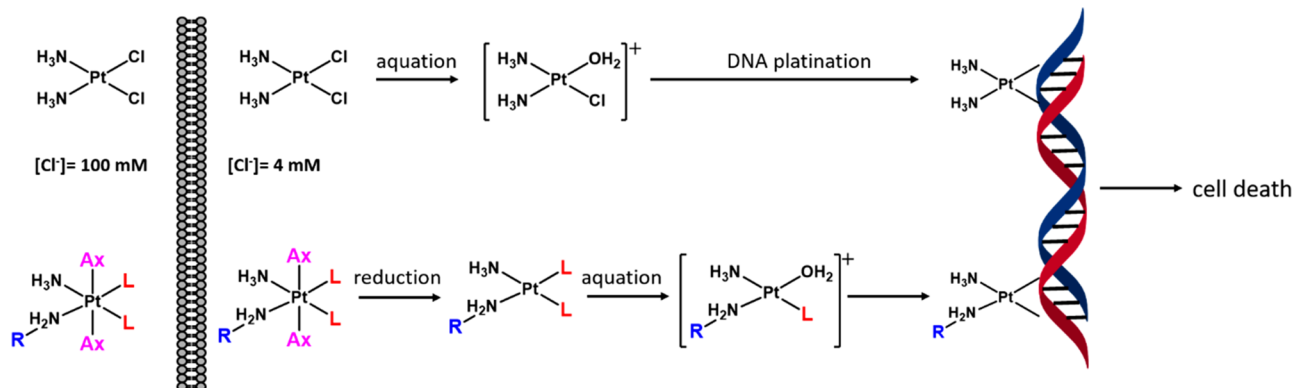
Herein we synthesized dual- and triple-action Pt(IV) derivatives of *cis*-[Pt(NH<sub>3</sub>)(CHA)(OAc)<sub>2</sub>]. These Pt(IV) compounds are analogues of satraplatin where the equatorial chlorides of satraplatin were replaced by acetates and the axial positions were functionalized with HDAC or PDK inhibitors. This generates novel complexes, where a single molecule can deliver multiple drugs having different target sites upon activation of the prodrug.

## EXPERIMENTAL SECTION

**Materials and Methods.** All of the chemicals and solvents were procured from reputed commercial sources and used without further purification.

Reaction mixtures were analyzed by an analytical HPLC system (Thermo Scientific UltiMate 3000) with a reverse-phase C18 column (Phenomenex Kinetex, length 250 mm, internal diameter 4.60 mm, particle size 5 μm, pore size 100 Å). The purity and retention time (RT) of Pt(IV) complexes reported here were measured with the aforementioned analytical HPLC system. The samples were dissolved in either methanol or acetonitrile and eluted with a 0–90% linear gradient of acetonitrile in water for 30 min under the detection of UV wavelengths at 220 and 260 nm. Bulk purification of the complexes was done using a preparative HPLC system (Thermo Scientific UltiMate 3000) attached with a reverse-phase C18 column (Phenomenex Luna, Length 250 mm, internal diameter 21.20 mm, particle size 10 μm, pore size 100 Å) following the same acetonitrile/water gradient mentioned above. UV detection was monitored at 220

**Scheme 1.** (Top) Labile Cisplatin Is Stabilized from Aquation Outside the Cell by the High Chloride Concentration and Once Inside the Cell Is Activated by Aquation That Facilitates DNA Binding and (Bottom) Inert Pt(IV) Is Stable Outside the Cell, and Once Inside, It Is Activated by Reduction That Is Followed by Aquation<sup>a</sup>



<sup>a</sup>Pt(IV) complexes do not depend on chloride concentrations for activation; thus, L can be a non-chloride ligand that undergoes aquation.

nm. Collected pure fractions were combined and lyophilized. All of the NMR data were recorded with a Bruker AVANCE IIIHD 500 MHz spectrometer. All of the data were processed with Bruker TopSpin 3.5pl7 software, and the chemical shifts were described in parts per million (ppm).  $^1\text{H}$  and  $^{13}\text{C}$  (proton decoupled) NMR chemical shifts were referenced with the individual solvent residual peaks of the respective NMR solvents used. Proton-decoupled  $^{195}\text{Pt}$  NMR chemical shifts were reported with respect to the chemical shift of the standard  $\text{K}_2\text{PtCl}_4$  in water at  $-1624$  ppm. Electrospray ionization mass spectra (ESI-MS) were measured using a Thermo Scientific triple-quadrature mass spectrometer (Quantum Access) by positive mode electrospray ionization. Elemental analyses reported were performed using a Thermo Scientific FLASH 2000 element analyzer.

**Synthesis.** *cis*-[Pt(NH<sub>3</sub>)(CHA)(OAc)<sub>2</sub>]. Silver acetate (369 mg, 2.21 mmol) was added to a solution of *cis*-[Pt(NH<sub>3</sub>)(CHA)I<sub>2</sub>]<sup>18</sup> (673 mg, 1.19 mmol; CHA = NH<sub>2</sub>C<sub>6</sub>H<sub>11</sub>) in 12 mL of DMF. After the mixture was stirred for 14 h at room temperature, precipitated AgI was filtered off and the filtrate was evaporated to give a brown oil. The oily residue was dissolved in a minimum volume of dichloromethane and precipitated with petroleum ether to afford a white solid of the required *cis*-diacetato Pt(II) complex. The color of the complex changes very quickly from white to light brown on exposure to light and therefore was quickly used for the next reaction. Yield: 430 mg (84%).  $^1\text{H}$  NMR (500 MHz, DMF-*d*<sub>7</sub>):  $\delta$  6.26 (br, 2H, NH<sub>2</sub>), 4.93 (br, 3H, NH<sub>3</sub>), 2.49 (m, 1H, H1), 2.32 (m, 2H, H2), 1.75 (s, 3H, OCOCH<sub>3</sub>), 1.73 (s, 3H, OCOCH<sub>3</sub>), 1.69 (m, 2H, H3), 1.56 (m, 1H, H4), 1.29–1.20 (m, 4H, H2 and H3), 1.09 (m, 1H, H4).  $^{13}\text{C}$  NMR (125 MHz, DMF-*d*<sub>7</sub>):  $\delta$  180.3 and 179.7 (OCOCH<sub>3</sub>), 56.5 (C1), 34.6 (C2), 26.5 (C4), 25.8 (C3), 24.3 and 24.2 (OCOCH<sub>3</sub>).  $^{195}\text{Pt}$  NMR (107.5 MHz, DMF-*d*<sub>7</sub>):  $\delta$   $-1623.4$ .

*cct*-[Pt(NH<sub>3</sub>)(CHA)(OAc)<sub>2</sub>(OH)] (1). A 20 mL portion of H<sub>2</sub>O<sub>2</sub> (30% w/v in water) was added to *cis*-[Pt(NH<sub>3</sub>)(CHA)(OAc)<sub>2</sub>] (220 mg, 0.51 mmol) at room temperature. The white solid dissolved quickly to give a yellow solution. The solution was stirred for another 14 h, after which H<sub>2</sub>O<sub>2</sub> was evaporated to dryness in a stream of compressed air to give a yellow oil. Diethyl ether was added followed by sonication and scratching, resulting in a yellow precipitate. Yield: 220 mg (93%). The crude powder was used for the next reactions without purification. For biological studies, the crude product was purified by HPLC (RT 10.2 min) to get 1 (purity >96%) as a yellow crystalline solid. Yield: 63 mg (26.5%).  $^1\text{H}$  NMR (500 MHz, MeOD):  $\delta$  2.76 (m, 1H, H1), 2.10–2.05 (m, 8H, H2 and 2  $\times$  OCOCH<sub>3</sub>), 1.78 (m, 2H, H3), 1.67 (m, 1H, H4), 1.37–1.19 (m, 5H, H2, H3 and H4).  $^{13}\text{C}$  NMR (125 MHz, MeOD):  $\delta$  182.66 and 182.61 (OCOCH<sub>3</sub>), 54.5 (C1), 34.1 and 33.6 (C2), 26.4 (C4), 26.11 and 26.05 (C3), 24.0 and 23.5 (OCOCH<sub>3</sub>).  $^{195}\text{Pt}$  NMR (107.5 MHz, MeOD):  $\delta$  1859.8. ESI-MS: calculated for [C<sub>10</sub>H<sub>24</sub>N<sub>2</sub>O<sub>6</sub>Pt + H]<sup>+</sup> 464.14, found 463.97. Anal. Calcd for C<sub>10</sub>H<sub>24</sub>N<sub>2</sub>O<sub>6</sub>Pt·H<sub>2</sub>O: C, 24.95; H, 5.44; N, 5.82. found: C, 24.82; H, 5.22; N, 6.15.

*cct*-[Pt(NH<sub>3</sub>)(CHA)(OAc)<sub>2</sub>(OAc)] (2). Excess acetic anhydride was added to a solution of 1 (250 mg, 0.54 mmol) in DMF (5 mL). The mixture was heated at 60 °C with stirring for 8 h. After completion of the reaction (as indicated by  $^{195}\text{Pt}$  NMR of the reaction mixture), the solution was centrifuged and the filtrate was evaporated completely in a rotary evaporator to give a yellow oil, which was purified by HPLC to yield 2 (RT 12.1 min, purity >99%) as an off-white solid. Yield: 70 mg (23.5%).  $^1\text{H}$  NMR (500 MHz, MeOD):  $\delta$  2.67 (m, 1H, H1), 2.09–2.03 (m, 14H, 4  $\times$  OCOCH<sub>3</sub> and H2), 1.77 (m, 2H, H3), 1.66 (m, 1H, H4), 1.35–1.26 (m, 4H, H2 and H3), 1.20 (m, 1H, H4).  $^{13}\text{C}$  NMR (125 MHz, MeOD):  $\delta$  182.2 (2  $\times$  OCOCH<sub>3</sub>, Axial), 181.29 and 181.15 (OCOCH<sub>3</sub>, Equatorial), 56.5 (C1), 33.2 (C2), 26.3 (C4), 26.2 (C3), 23.7 and 23.1 (OCOCH<sub>3</sub>, Equatorial), 22.3 (2  $\times$  OCOCH<sub>3</sub>, Axial).  $^{195}\text{Pt}$  NMR (107.5 MHz, MeOD):  $\delta$  2116.9. ESI-MS: calculated for [C<sub>14</sub>H<sub>28</sub>N<sub>2</sub>O<sub>8</sub>Pt + Na]<sup>+</sup> 570.14, found 569.94. Anal. Calcd for C<sub>14</sub>H<sub>28</sub>N<sub>2</sub>O<sub>8</sub>Pt: C, 30.71; H, 5.16; N, 5.12. Found: C, 30.63; H, 5.24; N, 5.02.

*cct*-[Pt(NH<sub>3</sub>)(CHA)(OAc)<sub>2</sub>(PhB)] (3). 4-Phenylbutyric acid anhydride (777 mg, 2.5 mmol) was added to a solution of 1 (145 mg, 0.31 mmol) in 6.5 mL of DMF. After it was stirred for 12 h at room

temperature, the reaction mixture was dried completely and purified by HPLC to give 3 (RT 26.7 min, purity >99%) as a yellow sticky gum. Yield: 50 mg (21.3%).  $^1\text{H}$  NMR (500 MHz, MeOD):  $\delta$  7.24–7.11 (m, 10H, CH<sub>PhB</sub>), 2.71–2.58 (m, 5H, H1 and  $^{\gamma}\text{CH}_2\text{PhB}$ ), 2.40–2.28 (m, 4H,  $^{\alpha}\text{CH}_2\text{PhB}$ ), 2.09–2.03 (m, 8H, H2 and 2  $\times$  OCOCH<sub>3</sub>), 1.94–1.82 (m, 4H,  $^{\beta}\text{CH}_2\text{PhB}$ ), 1.76 (m, 2H, H3), 1.64 (m, 1H, H4), 1.34–1.25 (m, 4H, H2 and H3), 1.19 (m, 1H, H4).  $^{13}\text{C}$  NMR (125 MHz, MeOD):  $\delta$  183.54 and 183.50 (C<sub>PhB</sub>), 182.3 and 181.4 (OCOCH<sub>3</sub>), 143.4 and 143.2 (C<sub>PhB</sub>), 129.62 and 129.57 (CH<sub>PhB</sub>), 129.30 and 129.26 (CH<sub>PhB</sub>), 126.83 and 126.76 (CH<sub>PhB</sub>), 56.4 (C1), 36.9 and 36.2 ( $^{\alpha}\text{CH}_2\text{PhB}$ ), 36.1 and 36.0 ( $^{\gamma}\text{CH}_2\text{PhB}$ ), 33.3 and 33.2 (C2), 29.2 and 28.9 ( $^{\beta}\text{CH}_2\text{PhB}$ ), 26.3 (C4), 26.1 (C3), 23.8 and 22.4 (OCOCH<sub>3</sub>).  $^{195}\text{Pt}$  NMR (107.5 MHz, MeOD):  $\delta$  2115.4. ESI-MS: calculated for [C<sub>30</sub>H<sub>44</sub>N<sub>2</sub>O<sub>8</sub>Pt + Na]<sup>+</sup> 778.26, found 778.06. Anal. Calcd for C<sub>30</sub>H<sub>44</sub>N<sub>2</sub>O<sub>8</sub>Pt: C, 47.68; H, 5.87; N, 3.71. Found: C, 47.98; H, 6.19; N, 3.84.

*cct*-[Pt(NH<sub>3</sub>)(CHA)(OAc)<sub>2</sub>(DCA)] (4). To a solution of 1 (160 mg, 0.34 mmol) in DMF (7 mL) was added dichloroacetic anhydride (320  $\mu\text{L}$ , 2.09 mmol) dropwise, and the mixture was stirred at room temperature for 14 h. Upon completion, the reaction mixture was evaporated to dryness and subsequent HPLC purification provided 4 (RT 20.5 min, purity >96%) as a very faint yellow powder. Yield: 50 mg (21.4%).  $^1\text{H}$  NMR (500 MHz, MeOD):  $\delta$  6.27 (s, 1H, OCOCHCl<sub>2</sub>), 6.26 (s, 1H, OCOCHCl<sub>2</sub>), 2.68 (m, 1H, H1), 2.14–2.05 (m, 8H, H2 and 2  $\times$  OCOCH<sub>3</sub>), 1.77 (m, 2H, H3), 1.66 (m, 1H, H4), 1.40–1.28 (m, 4H, H2 and H3), 1.20 (m, 1H, H4).  $^{13}\text{C}$  NMR (125 MHz, MeOD):  $\delta$  182.3 and 181.0 (OCOCH<sub>3</sub>), 172.60 and 172.57 (OCOCHCl<sub>2</sub>), 67.2 and 66.2 (OCOCHCl<sub>2</sub>), 56.8 (C1), 33.4 and 32.6 (C2), 26.2 (C4), 26.15 and 26.06 (C3), 23.5 and 21.8 (OCOCH<sub>3</sub>).  $^{195}\text{Pt}$  NMR (107.5 MHz, MeOD):  $\delta$  2104.5. ESI-MS: calculated for [C<sub>14</sub>H<sub>24</sub>Cl<sub>2</sub>N<sub>2</sub>O<sub>8</sub>Pt + Na]<sup>+</sup> 706.98, found 706.71; Anal. Calcd for C<sub>14</sub>H<sub>24</sub>Cl<sub>2</sub>N<sub>2</sub>O<sub>8</sub>Pt: C, 24.54; H, 3.53; N, 4.09. Found: C, 24.86; H, 3.72; N, 4.09.

*cct*-[Pt(NH<sub>3</sub>)(CHA)(OAc)<sub>2</sub>(PhB)(OH)] (5). *cis*-[Pt(NH<sub>3</sub>)(CHA)(OAc)<sub>2</sub>] (230 mg, 0.53 mmol) and 4-phenylbutyric acid (1.7 g, 10.3 mmol) were allowed to dissolve completely in 6 mL of THF, and to this solution was added H<sub>2</sub>O<sub>2</sub> (150  $\mu\text{L}$ , 1.32 mmol) dropwise. The yellow reaction mixture was stirred for 14 h at room temperature and then heated at 45 °C for another 36 h. After that THF was evaporated and the resulting oil was dissolved in a minimum volume of diethyl ether to which a large volume of petroleum ether was added. The whole mixture was refrigerated for 0.5 h and centrifuged to give a brown oil at the bottom of the centrifuge tube. The brown oil was preserved, discarding the other liquid on top of it. This procedure was repeated three times to yield crude 5. Further HPLC purification was performed to give 5 (RT 17.9 min, purity >98%) as a white powder. Yield: 70 mg (20.7%).  $^1\text{H}$  NMR (500 MHz, MeOD):  $\delta$  7.26–7.18 (m, 4H, CH<sub>PhB</sub>), 7.15–7.12 (m, 1H, CH<sub>PhB</sub>), 2.72–2.60 (m, 3H, H1 and  $^{\gamma}\text{CH}_2\text{PhB}$ ), 2.35 (t,  $J$  = 7.28 Hz, 2H,  $^{\alpha}\text{CH}_2\text{PhB}$ ), 2.21–1.97 (m, 8H, H2 and 2  $\times$  OCOCH<sub>3</sub>), 1.92–1.86 (m, 4H,  $^{\beta}\text{CH}_2\text{PhB}$ ), 1.77 (m, 2H, H3), 1.66 (m, 1H, H4), 1.39–1.26 (m, 4H, H2 and H3), 1.21 (m, 1H, H4).  $^{13}\text{C}$  NMR (125 MHz, MeOD):  $\delta$  184.3 (C<sub>PhB</sub>), 182.6 and 182.3 (OCOCH<sub>3</sub>), 143.4 (C<sub>PhB</sub>), 129.5 (CH<sub>PhB</sub>), 129.2 (CH<sub>PhB</sub>), 126.7 (CH<sub>PhB</sub>), 55.7 (C1), 37.3 ( $^{\alpha}\text{CH}_2\text{PhB}$ ), 36.1 ( $^{\gamma}\text{CH}_2\text{PhB}$ ), 33.5 and 33.1 (C2), 29.0 ( $^{\beta}\text{CH}_2\text{PhB}$ ), 26.3 (C4), 26.1 and 26.0 (C3), 24.1 and 23.3 (OCOCH<sub>3</sub>).  $^{195}\text{Pt}$  NMR (107.5 MHz, MeOD):  $\delta$  1936.6. ESI-MS: calculated for [C<sub>20</sub>H<sub>34</sub>N<sub>2</sub>O<sub>7</sub>Pt + H]<sup>+</sup> 610.21, found 609.99. Anal. Calcd for C<sub>20</sub>H<sub>34</sub>N<sub>2</sub>O<sub>7</sub>Pt: C, 39.41; H, 5.62; N, 4.60. Found: C, 40.02; H, 5.66; N, 4.56.

*cct*-[Pt(NH<sub>3</sub>)(CHA)(OAc)<sub>2</sub>(PhB)(DCA)] (6). Crude 5 (500 mg, 0.82 mmol) in 2 mL of DMF, as received from the previous reaction, was reacted with dichloroacetic anhydride (480  $\mu\text{L}$ , 3.15 mmol). After accomplishment of the reaction, the mixture was dried. Purification by HPLC gave 6 (RT 23.7 min, purity >97%) as a light yellow fluffy powder. Yield: 120 mg (20.2%).  $^1\text{H}$  NMR (500 MHz, MeOD):  $\delta$  7.26–7.18 (m, 4H, CH<sub>PhB</sub>), 7.16–7.13 (m, 1H, CH<sub>PhB</sub>), 6.26–6.25 (d, 1H, CH<sub>DCA</sub>), 2.72–2.61 (m, 3H, H1 and  $^{\gamma}\text{CH}_2\text{PhB}$ ), 2.41–2.31 (m, 2H,  $^{\alpha}\text{CH}_2\text{PhB}$ ), 2.10–2.04 (m, 8H, H2 and 2  $\times$  OCOCH<sub>3</sub>), 1.92–1.83 (m, 2H,  $^{\beta}\text{CH}_2\text{PhB}$ ), 1.75 (m, 2H, H3), 1.63 (m, 1H, H4), 1.34–1.26 (m, 4H, H2 and H3), 1.20 (m, 1H, H4).  $^{13}\text{C}$  NMR (125 MHz,

MeOD):  $\delta$  183.5 and 183.2 ( $\text{CO}_{\text{phB}}$ ), 182.39 and 182.36 ( $\text{OCOCH}_3$ , Axial), 181.3 and 181.0 ( $\text{OCOCH}_3$ , Equatorial), 172.49 and 172.48 ( $\text{OCOCHCl}_2$ ), 143.4 and 143.2 ( $\text{C}_{\text{phB}}$ ), 129.64 and 129.57 ( $\text{CH}_{\text{phB}}$ ), 129.3 and 129.2 ( $\text{CH}_{\text{phB}}$ ), 126.8 and 126.7 ( $\text{CH}_{\text{phB}}$ ), 66.34 and 66.31 ( $\text{OCOCHCl}_2$ ), 56.4 and 56.3 (C1), 36.8 and 35.7 ( $^{\alpha}\text{CH}_{2\text{phB}}$ ), 36.09 and 36.06 ( $^{\beta}\text{CH}_{2\text{phB}}$ ), 33.59 and 33.54 (C2), 32.75 and 32.71 (C2), 29.1 and 28.8 ( $^{\beta}\text{CH}_{2\text{phB}}$ ), 26.3 and 26.2 (C4), 26.2 and 26.1 (C3), 23.6 and 23.1 ( $\text{OCOCH}_3$ , Equatorial), 21.9 ( $\text{OCOCH}_3$ , Axial).  $^{195}\text{Pt}$  NMR (107.5 MHz, MeOD):  $\delta$  2116.1. ESI-MS: calculated for  $[\text{C}_{22}\text{H}_{34}\text{Cl}_2\text{N}_2\text{O}_8\text{Pt} + \text{Na}]^+$  742.12, found 742.92. Anal. Calcd for  $\text{C}_{22}\text{H}_{34}\text{Cl}_2\text{N}_2\text{O}_8\text{Pt}$ : C, 36.67; H, 4.76; N, 3.89. Found: C, 36.81; H, 4.80; N, 3.98.

**Determination of Water Solubility.** In order to determine the water solubility of the synthesized Pt(IV) complexes, the standard shake flask method was followed. In brief, saturated water solutions of each complex were prepared by shaking for 24 h in water at room temperature. After that, each solution was filtered and injected into an analytical HPLC. The unknown concentrations of complexes in water were calculated from the standard curve of the respective complexes.

**Stability in Phosphate Buffer.** The stability of the Pt(IV) complexes (except complex 3) were studied in 50 mM phosphate buffer (pH 7.0) at 37 °C. Due to low aqueous solubility, the study of complex 3 was performed in a 20% mixture of MeCN in 50 mM phosphate buffer (pH 7.0).

Briefly, the Pt(IV) complexes were incubated at 37 °C in the dark and injected into analytical HPLC at different time intervals. The samples were run in a linear gradient of 0–90% acetonitrile in water over 30 min. The half-lives ( $t_{1/2}$ ) were determined after linear fitting of  $\ln(A_t/A_0)$  vs time ( $t$ ) by considering a pseudo-first-order rate equation for the hydrolysis ( $A_t = A_0e^{-kt}$ ; eq 1), where  $A_0$  and  $A_t$  are the integrated areas of HPLC peaks of the respective complexes at  $t = 0$  and at time  $t$ , respectively, and  $k$  is the rate constant. Then the  $t_{1/2}$  value was calculated by utilizing the equation  $t_{1/2} = 0.693/k$ .

**Rates of Reduction.** This study was performed using the same experimental conditions as those for the stability study in phosphate buffer (50 mM) with addition of 10 equiv of L-ascorbic acid (pH 7). The decreasing intensities of the respective peaks of the Pt(IV) complexes were monitored with analytical HPLC, and  $t_{1/2}$  values were determined following eq 1 above.

**Cell Lines and Culture Conditions.** The human and murine cancer cell lines used in this study are summarized together with the source and respective growth medium in Table S1. All media were supplemented with 10% fetal bovine serum. Cultures were regularly checked for mycoplasma contamination. Cultures were maintained at 37 °C in a humidified atmosphere containing 95% air and 5%  $\text{CO}_2$ .

**Cytotoxicity Tests in Cancer Cell Lines.** To determine cell viability,  $(2-5) \times 10^4$  cells/mL (depending on the proliferation speed of the cell line) were seeded in 96-well plates (100  $\mu\text{L}$ /well) and allowed to recover for 24 h. Then, cells were exposed to the test drugs at the indicated concentrations for 72 h. Anticancer activity was measured by the 3-(4,5-dimethylthiazol-2-yl)-2,5-diphenyltetrazolium bromide (MTT) based vitality assay (EZ4U; Biomedica, Vienna, Austria) following the manufacturer's recommendations. Cytotoxicity was calculated using the GraphPad Prism software (using a point-to-point function) and was expressed as  $\text{IC}_{50}$  values calculated from full dose–response curves (drug concentrations inducing a 50% reduction of cell number in comparison to untreated control cells cultured in parallel).

**Total Pt Uptake Levels.** CT26 cells ( $5 \times 10^5$ /well) were drug-exposed for 3 h at 37 °C. After two washing steps with PBS, cells were lysed at room temperature in 500  $\mu\text{L}$  of 67–69%  $\text{HNO}_3$  (83872.270, VWR) for 1 h. A 400  $\mu\text{L}$  portion of the lysate was added to 7.6 mL of distilled deionized water, and platinum concentrations were determined by ICP-MS using an Agilent 7800 ICP-MS instrument. The ICP-MS Agilent 7800 instrument (Agilent Technologies, Tokyo, Japan) was equipped with a CETAC ASX-520 autosampler (Nebraska, USA) and a MicroMist nebulizer at a sample uptake rate of approximately 0.2 mL/min. The Agilent MassHunter software package (Workstation Software, version C.01.04, Build 544.17, Patch 3, 2018) was used for data processing. As unspecific binding to cell

culture plastic may occur especially in case of lipophilic compounds;<sup>47</sup> therefore, results were corrected for platinum levels of a blank well containing no cells.

**Time-Lapse Microscopy.** Cells in an amount of  $4 \times 10^4$  cells/well were seeded in an 8-well  $\mu$ -slide (ibidi, Martinsried, Germany) and allowed to recover for 24 h. The cells were treated with the respective compounds at 5  $\mu\text{M}$ , and the image series was started directly after treatment in a humidified incubation chamber (37 °C, 5%  $\text{CO}_2$ ) on a LiveCell Inverted Brightfield Microscope Nikon Eclipse Ti (20x Super Plan Fluor NA 0.45 Ph1, PCS sCMOS monochrome camera 4.2MPxl, rolling shutter, Visiview Software).

**Morphological Evaluation of CT26 Cells.** Briefly,  $2 \times 10^5$  cells were seeded in 6-well plates, allowed to recover for 48 h, and treated for another 24 h. Subsequently, cells were collected and cytopins prepared using a cytocentrifuge (Cytospin 4, Thermo Scientific, Waltham, MA, USA) at 400 rpm for 5 min. After fixation with methanol/acetone (–20 °C, 1/1) cells were stained with 4',6-diamidino-2'-phenylindole dihydrochloride (DAPI). For each slide, 200–300 nuclei were scored normal, mitotic, or apoptotic.

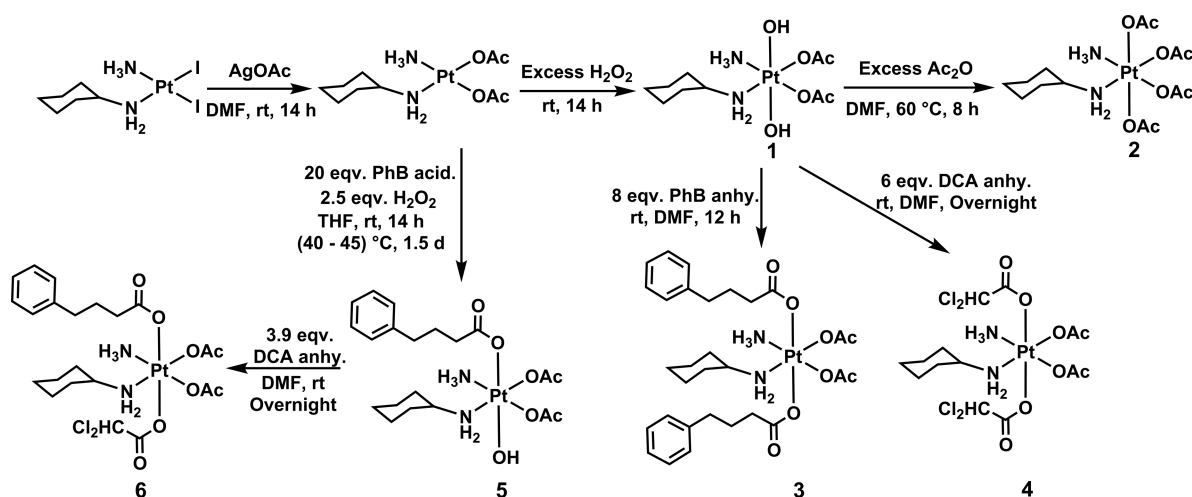
**Cell Cycle Analysis by Flow Cytometry.** CT26 cells were seeded in 6-well plates at a density of  $3 \times 10^5$  cells. Cells were treated at 1 and 2  $\mu\text{M}$  concentrations for 24 h and subsequently trypsinized, washed with PBS, and fixed in 70% ethanol (1 h at –20 °C). Fixed cells were centrifuged (8 min, 6000g) and resuspended in 100  $\mu\text{L}$  of 0.9% NaCl, and RNA was digested with 0.2 mg/mL RNase for 30 min at 37 °C. Nuclei were stained with propidium iodide (PI, 0.01 mg/mL, Sigma-Aldrich, St. Louis, MO, USA) for 30 min at 4 °C in the dark. Cells were analyzed by flow cytometry using a BD LSR Fortessa™ instrument, and FlowJo software was used to evaluate the results.

**Immunofluorescence (DNA Damage).** Cells in an amount of  $4 \times 10^3$  CT26 cells were seeded on "PTFE"-printed slides (E63424-06, Science Services). After 24 h of recovery cells were treated for 19 h and subsequently fixed in 4% paraformaldehyde (PFA) solution for 10 min at room temperature before washing two times for 1 min in PBS. Cells were incubated with blocking buffer (5% BSA, 0.2% Triton X, in PBS) and subsequently incubated with antiphospho-H2AX antibody (cell signaling (20E3) #9718, 1/200 diluted in PBS with 1% BSA and 0.2% Triton X) for 1 h at room temperature. After two further washing steps with PBS, cells were incubated (1 h) with the secondary antibody (antirabbit IgG labeled with FITC, Sigma-Aldrich) and with phalloidin-tetramethylrhodamine B isothiocyanate (phalloidin TRITC, P1951, Sigma) 1/500 and 1/1000 diluted in PBS with 1% BSA and 0.2% Triton X. Cells were counterstained with DAPI before mounting. Images were obtained using a Zeiss LSM 700 confocal microscope (Plan-Apochromat 63x/1.4 Oil DIC M27 LSM 700 AxioObserver). Subsequent image handling was carried out using ImageJ software. The nuclei area from each image was selected and used to detect the sum of the pixel values in the pH2AX channel (integrated density). Integrated density was normalized to nuclei area. From each condition eight images were quantified.

**Immunohistochemistry (DNA Damage).** Immunohistochemistry was performed according to the standard procedure. Shortly, 4  $\mu\text{m}$  sections of paraffin-embedded tumor samples were deparaffinized, blocked for endogenous peroxidase by incubating for 10 min in tris-buffered saline 0.3%  $\text{H}_2\text{O}_2$ , and rehydrated. Antigens were retrieved by boiling the samples in 10 mM citrate buffer (pH 6.0) for 3 min at 1.5 bar. The samples were blocked using Ultra V Block (UltraVision LP) and subsequently incubated with the primary antibody against pH2AX (Cell Signaling, #9718, 1/1000). Antibody binding was detected by HRP polymers (UltraVision LP), and the color was developed using 3,3'-diaminobenzidine. Samples were counterstained with hematoxylin.

**Animal Experiments.** All animal experiments were approved by the local ethics commission and carried out according to the Austrian and FELASA guidelines for animal care and protection. Eight- to twelve-week-old female BALB/c mice (weighing ~20 g) were purchased from Envigo, Italy. The animals were kept in a pathogen-free environment, and every procedure was done in a laminar airflow cabinet.

Scheme 2. Synthetic Scheme for the Preparation of Equatorial Acetate Modified Dual- and Triple-Action Satraplatin Derivatives



**Anticancer Activity against CT-26 Cells in Vivo.** Murine CT-26 cells ( $5 \times 10^5$ ) were injected subcutaneously into the right flank of female BALB/c mice. Animals were treated with the drug (dissolved in 5% DMSO) either intraperitoneally or orally at the indicated drug concentrations at day 4, 6, 8, 11, 13, and 15. Animals were controlled for distress development every day, and the tumor size was assessed regularly by caliper measurement. Tumor volume was calculated using the formula  $(\text{length} \times \text{width})^2/2$ .

## RESULTS AND DISCUSSION

**Synthesis and Chemical Characterization.** The synthesis of the target compounds, dual- and triple-action Pt(IV)

**Table 1. Chemical Properties of Compounds 1–6: Water Solubility, Stability in Phosphate Buffer, and Half-Lives in Ascorbic Acid**

complex	water solubility (mg/mL) <sup>a</sup>	half-life in phosphate buffer $t_{1/2}$ (day) <sup>b</sup>	half-life with 10 equiv L-ascorbic acid $t_{1/2}$ (h) <sup>c</sup>
1	>2	16.5 <sup>b</sup>	0.4 <sup>b</sup>
2	>2 (>3.6 mM)	9.6 <sup>b</sup>	35.9 <sup>b</sup>
3	0.006–0.02	18.5 <sup>c</sup>	151.9 <sup>c</sup>
4	1.26–1.83	0.04 <sup>b</sup>	1 <sup>b</sup>
5	0.10–0.12	23.9 <sup>b</sup>	0.5 <sup>b</sup>
6	0.37–0.71	8.2 <sup>b</sup>	15.9 <sup>b</sup>
satraplatin	0.4 (0.8 mM)	3.1 <sup>c</sup>	0.8 <sup>c</sup>

<sup>a</sup>24 h in water at room temperature <sup>b</sup>50 mM phosphate buffer pH 7.0 at 37 °C. <sup>c</sup>20% MeCN in 50 mM phosphate buffer pH 7.0 at 37 °C.

derivatives of satraplatin with axial acetato ligands, proceeded according to Scheme 2. Initially, the precursor, *cis*-[Pt(NH<sub>3</sub>)(CHA)<sub>2</sub>I<sub>2</sub>], was synthesized from *cis*-[Pt(CHA)<sub>2</sub>I<sub>2</sub>], following the procedure of Lippard et al.<sup>18</sup> The iodides were replaced with acetates by reacting *cis*-[Pt(NH<sub>3</sub>)(CHA)I<sub>2</sub>] with 2 equiv of Ag(OAc) in the polar aprotic solvent DMF. The desired compound, *cis*-[Pt(NH<sub>3</sub>)(CHA)(OAc)<sub>2</sub>], was obtained as a white powder in 84% yield. <sup>195</sup>Pt NMR of the reaction mixture indicated a shift of the resonance at  $-3307.7$  ppm (starting *cis*-diiododiam(m)ine Pt(II) complex, data not shown) to  $-1623.4$  ppm (Figure S1A). This chemical shift indicates that two oxygen atoms are bound to the *cis*-diam(m)ine Pt(II) center. Two acetate singlets at 1.75 and 1.73 ppm in the <sup>1</sup>H

NMR (DMF-*d*<sub>7</sub>) corresponding to the two methyl groups of the acetates confirm the binding to the platinum (Figure S1B). These data also correlate with their <sup>13</sup>C NMR chemical shifts at 24.2 and 24.1 ppm, respectively, in DMF-*d*<sub>7</sub>, and the carbonyl <sup>13</sup>C chemical shifts were found at 180.3 and 179.7 ppm, respectively (Figure S1C,D). The NH<sub>2</sub> and NH<sub>3</sub> groups gave two broad signals at 6.26 and 4.93 ppm, respectively, in the <sup>1</sup>H NMR (Figure S1B). Among the protons of the cyclohexyl group, the H1 proton (attached to NH<sub>2</sub>) possesses the most downfield chemical shift at 2.49 ppm as a one-proton multiplet. Then the chemical shifts for H2, H3, and H4 came in a descending order of sequence (Figure S1B). However, they came in two different sets, in accordance with their axial and equatorial positions. In <sup>13</sup>C NMR the sequence changed as the chemical shift corresponding to C4 came before that of C3 (Figure S1C).

*cis*-[Pt(NH<sub>3</sub>)(CHA)(OAc)<sub>2</sub>] was oxidized readily to the Pt(IV) complex **1** with 30% H<sub>2</sub>O<sub>2</sub> (Scheme 2). Apart from a color change (to yellow), the <sup>195</sup>Pt NMR chemical shift at  $\sim 1860$  ppm (Figure S2A) confirmed the oxidation to the Pt(IV) species *cct*-[Pt(NH<sub>3</sub>)(CHA)(OAc)<sub>2</sub>(OH)<sub>2</sub>]. This complex is inert and hence was purified by reverse-phase HPLC using a MeCN/water gradient (Figure S2B) and was characterized by ESI-MS (Figure S2C) and NMR (Figure S2D,E); its purity was confirmed by elemental analysis. The NMR, ESI-MS, and elemental analysis support the formation of **1**.

We acetylated both axial positions of **1** with an excess of acetic anhydride to produce the Pt(IV) complex **2** (*cct*-[Pt(NH<sub>3</sub>)(CHA)(OAc)<sub>2</sub>(OAc)<sub>2</sub>]; Scheme 2). **2** differs from satraplatin only by replacement of the chlorido ligands by acetates. The <sup>195</sup>Pt NMR spectrum of **2** has a resonance at 2116.9 ppm (Figure S3A), indicating bis-acetylation. Both axial methyl groups have the same chemical shifts at 2.03 ppm in the <sup>1</sup>H NMR (Figure S3C). This is also true in the <sup>13</sup>C NMR, where both of the methyl carbons resonate at 22.2 ppm and the carbonyls at 182.1 ppm (Figure S3D). Put together, we conclude that the axial acetates of **2** are equivalent.

We prepared dual-action Pt(IV) complexes by esterifying the two axial OH groups of **1** with PhB anhydride or DCA anhydride to generate complexes **3** and **4**, respectively (Scheme 2). The two PhB ligands in the two axial positions

Table 2. Cytotoxicity Assessed by MTT Assay<sup>a</sup>

drug	IC <sub>50</sub> (μM)							
	HCT-116	A2780	CT-26	B-16	SW480	Capan-1	p31	DU145
CisPt	5.4 ± 0.30	1.6 ± 0.57	3.9 ± 1.42	9.6 ± 3.70	7.1 ± 0.40	9.3 ± 4.83	15.4 ± 8.1	1.3 ± 0.89
SatrapPt	4.0 ± 0.60	3.4 ± 2.44	5.5 ± 2.19	4.0 ± 0.75	3.6 ± 0.14	6.4 ± 3.64	8.0 ± 1.28	3.3 ± 0.77
1	45.5 ± 3.34	20.6 ± 9.59	37.2 ± 7.66	>100	20.7 ± 2.89	>100	96.2 ± 24.08	21.8 ± 0.94
2	39.4 ± 3.15	24.1 ± 7.74	49.2 ± 4.53	>100	43.9 ± 8.39	>100	89.9 ± 26.35	27.4 ± 5.51
3	0.4 ± 0.05	0.2 ± 0.05	1.3 ± 0.07	0.5 ± 0.08	0.6 ± 0.13	0.6 ± 0.32	0.6 ± 0.00	0.3 ± 0.05
4	1.2 ± 0.20	0.6 ± 0.24	2.1 ± 0.20	1.0 ± 0.11	1.2 ± 0.20	2.1 ± 1.36	1.7 ± 0.16	1.1 ± 0.21
5	0.4 ± 0.12	0.2 ± 0.04	5.3 ± 0.51	1.1 ± 0.11	0.8 ± 0.38	0.3 ± 0.03	0.5 ± 0.06	0.3 ± 0.02
6	0.3 ± 0.05	0.2 ± 0.08	1.0 ± 0.02	0.3 ± 0.02	0.4 ± 0.03	0.3 ± 0.12	0.4 ± 0.19	0.3 ± 0.02

<sup>a</sup>Cells were treated for 72 h with increasing concentrations of test compounds. IC<sub>50</sub> values (given as mean ± SD) indicate the concentration yielding a 50% reduction in cell viability.

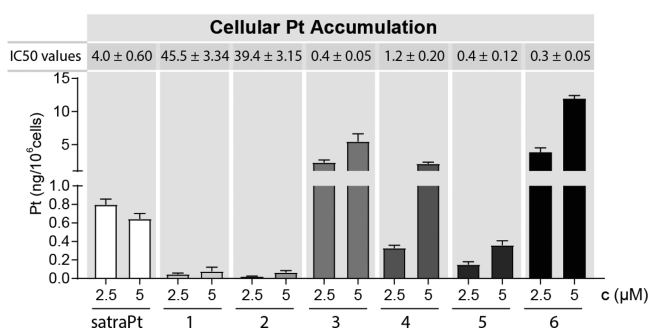


**Figure 2.** Intracellular platinum accumulation of the investigated complexes. CT-26 cells were treated with the indicated drugs at 2.5 or 5 μM for 3 h at 37 °C. Intracellular platinum levels were detected by ICP-MS measurements. Bars depict platinum amount (in ng) per 10<sup>6</sup> cells as mean ± SD (*n* = 3) of one representative experiment.

of **3** are not magnetically equivalent, as is reflected in their chemical shifts in <sup>1</sup>H (Figure S4B) and <sup>13</sup>C (Figure S4C,D) NMR. The HPLC chromatogram has a single peak with a purity of >99% (Figure S4E). This suggests that there might not be free rotation around the Pt–PhB bonds due to the CHA ligand. Similarly, the protons of axial DCA in **4** are slightly separated, resonating at 6.27 and 6.26 ppm (Figure S5C). This is supported by <sup>13</sup>C NMR (67.2 and 66.2 ppm for the two DCA CH carbons and 172.6 and 172.5 ppm for DCA carbonyl carbons; Figure S5D). The lack of free rotation of the bulky axial ligands (PhB and DCA) is further supported by the fact that, with the exception of **2** which has small acetato ligands, the <sup>13</sup>C NMR of **3**–**6** show that each carbon in CHA has a unique chemical shift. This suggests that there is no free rotation of the CHA probably due to steric interactions with the axial ligands.

We tried to prepare the nonsymmetric Pt(IV) complexes by monocarboxylation of **1** with PhB (complex **5**) by reacting **1** with 1.2 equiv of PhB anhydride in DMSO. We monitored the progress of the reaction by <sup>195</sup>Pt NMR. After 20 h of stirring at room temperature, we observed two peaks at 1957.1 and 2159.1 ppm for unreacted bis-hydroxido (**1**) and the bis-carboxylato (**3**) Pt(IV) complexes, respectively (Figure S6A). Interestingly, there was no sign of any peak for the monocarboxylato (**5**) Pt(IV) at ca. 2000–2100 ppm. Repeating the reaction in DMF yielded the same result (Figure S6B).

Therefore, we tried to carry out the monocarboxylation of *cis*-[Pt(NH<sub>3</sub>)(CHA)(OAc)<sub>2</sub>(OH)<sub>2</sub>] with the help of a method previously reported by our group.<sup>48</sup> In this process, we began with the Pt(II) complex *cis*-[Pt(NH<sub>3</sub>)(CHA)(OAc)<sub>2</sub>] and

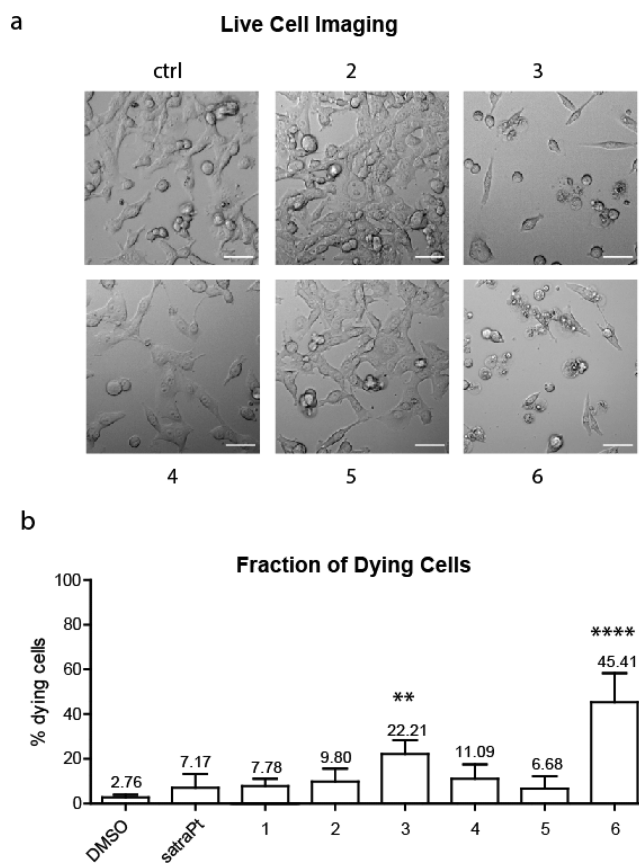


**Figure 3.** Morphological changes after drug treatment. (a) Images of CT-26 cells treated with the new complexes at 5 μM for 24 h. Images were taken by time-lapse microscopy (every 20 min). The scale bar is 100 μm. (b) CT-26 cells treated with 5 μM of the respective complexes for 24 h. Nuclei were stained by DAPI, and the morphology was analyzed. Cells from five representative images were quantified. Bars depict mean ± SD (percent of apoptotic cells is indicated above the respective bar). Significance (\*\**p* < 0.01, \*\*\*\**p* < 0.0001) in comparison to DMSO control was calculated by one-way ANOVA using GraphPad Prism software.

oxidized this complex with a slight excess of H<sub>2</sub>O<sub>2</sub> (2.5 equiv) in the presence of 20 equiv of PhB in THF (Scheme 2). After the reaction mixture was stirred overnight at room temperature, we observed two large peaks of almost equal intensity in <sup>195</sup>Pt NMR at 1947.3 and 2018.8 ppm and a very small signal at 2097.5 ppm (Figure S6C). The oxidation gave rise to two major products. The first peak is the usual H<sub>2</sub>O<sub>2</sub> oxidation product *cis*-[Pt(NH<sub>3</sub>)(CHA)(OAc)<sub>2</sub>(OH)<sub>2</sub>], and the second

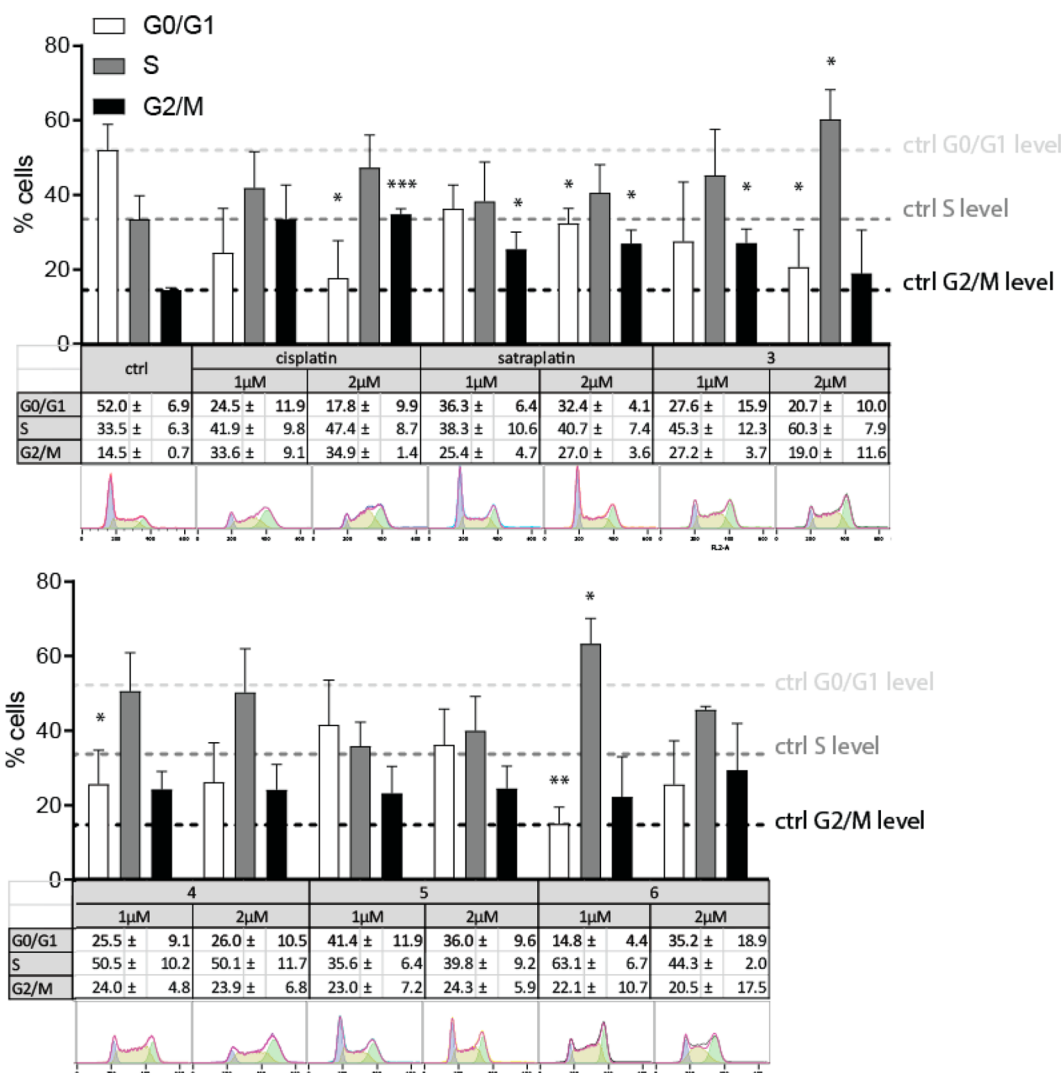


**Figure 4.** Changes in cell cycle distribution upon drug treatment in CT26 cells. Cell cycle analysis was done by flow cytometry determining the DNA content of the ethanol-fixed, PI-stained cells after 24 h of treatment with the indicated drug concentrations. Bars show percentages of cells in G0/G1, S, and G2/M phases of the cell cycle, calculated by FlowJo software and depicted as mean  $\pm$  SD; *p* values were calculated by multiple *t* test analysis (\**p* < 0.05, \*\**p* < 0.01, \*\*\**p* < 0.001). Individual values are given below.

peak corresponds to **5** with one axial OH (from H<sub>2</sub>O<sub>2</sub>) and one axial PhB. The minor peak results from the biscarboxylation: i.e., **3**. The reaction mixture was heated to 40–45 °C for another 1.5 days, upon which it yielded **5** as a major peak with **3** as a minor peak (Figure S6D). Here, we see that the PhB (acid) reacts with *cct*-[Pt(NH<sub>3</sub>)(CHA)(OAc)<sub>2</sub>(OH)<sub>2</sub>] directly upon prolonged heating, although in our earlier report<sup>49</sup> the heating of the reaction mixture was strictly prohibited. Warming the reaction mixture, in this case, yielded the desired product.

Compound **6** was prepared from **5** by esterification of the remaining OH group of **5** with DCA anhydride to yield the triple-action Pt(IV) complex **6** (Scheme 2). HPLC suggests the existence of two isomers of **6** at RT 23.7 min that cannot be separated (Figure S8A). The <sup>1</sup>H (Figure S8C) and <sup>13</sup>C NMR spectra (Figure S8D–H) were also in accordance with two isomers.

**Water Solubility.** One of the goals of replacing the chlorido ligands with acetato ligands was to try to increase the aqueous solubility. The enhancement in solubility gained by just replacing chlorides with acetates is evident when the

solubilities of satraplatin (0.4 mg/mL, 0.8 mM) and compounds **2** (>2 mg/mL, 3.6 mM) are compared. We determined the range of the water solubility of our complexes **1–6**, and the data are summarized in Table 1 in mg/mL. With the exception of **3** and **5**, all compounds are more soluble than satraplatin (0.4 mg/mL).

**Stability in Phosphate Buffer.** We examined the stability of our Pt(IV) complexes in 50 mM phosphate buffer at pH 7.0 and 37 °C, and the stability was monitored by HPLC and is expressed as half-life (*t*<sub>1/2</sub>) in Table 1.

Among all the complexes, **5** is the most and **4** is the least stable (Table 1). We assume that the main cause of instability is aquation—the replacement of one axial ligand by a hydroxide. Within less than 1 h (*t*<sub>1/2</sub> ≈ 0.9 h) half of **4** (RT 20.6 min) was hydrolyzed to produce the monohydroxido-mono-DCA derivative *cct*-[Pt(NH<sub>3</sub>)(CHA)(OAc)<sub>2</sub>(DCA)(OH)] (**4a**, RT 14.8 min; Figure S10A), which was characterized by ESI-MS, having an MH<sup>+</sup> peak at *m/z* 574.83 (calcd *m/z* 574.07; Figure S10B). This is in agreement with what we reported previously.<sup>49</sup> After 400 min only 0.5% of **4** remained intact (Figure S10C). Complex **6** with one DCA

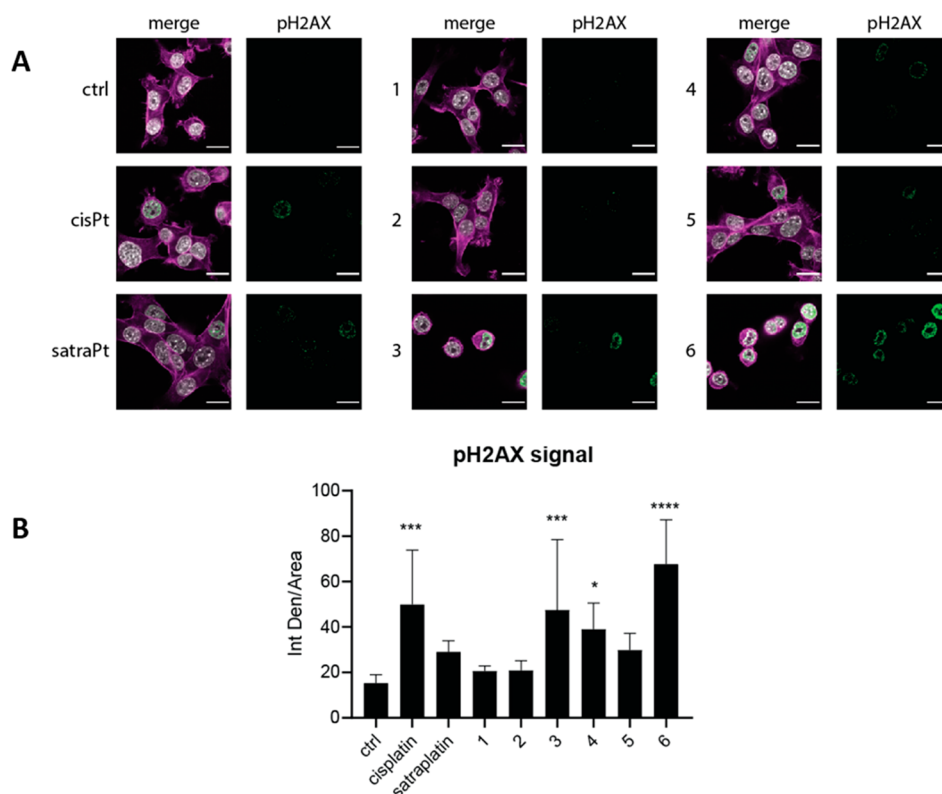


**Figure 5.** Induction of DNA damage by the compound panel. (A) CT26 cells treated with the respective compounds at 2.5  $\mu\text{M}$  for 19 h. Then cells were fixed with 4% PFA solution. Nuclei were stained with DS9API (depicted in gray), actin was stained with TRITC-phalloidin (depicted in magenta), and DNA damage was visualized by pH2AX staining (depicted in green). The scale bar is 20  $\mu\text{m}$ . (b) Integrated intensity of pH2AX signals from (a) quantified using ImageJ software. Bars present mean  $\pm$  SD ( $n = 8$ ). The significance in comparison to control samples was calculated by one-way ANOVA using GraphPad Prism software (\* $p < 0.05$ , \*\*\* $p < 0.001$ , \*\*\*\* $p < 0.0001$ ).

and one PhB attached to the axial position has a long half-life in buffer (8.2 days). The same is true for the tetraacetato complex **2** with a half-life of 9.6 days. The species found in addition to **2** (RT 12.1 min) in the HPLC are the hydrolysis products of the acetates at RT 11.7 and 9.1 min (Figure S12A,B). **1**, **3**, and **5** have half-lives greater than 15 days (Table 1) in buffer and hence their speciations are not discussed here. It is interesting and important to note that the bis-DCA compound **4** is significantly less stable than the mono-PhB-mono-DCA compound **6**, attesting to the strong influence of the electronic properties of the axial ligand on the rate of hydrolysis of the ligand trans to it.

**Rates of Reduction.** The design of Pt(IV) prodrugs is predicated on the assumption that they will remain intact in the bloodstream and will be reduced primarily inside the malignant tissue.<sup>51,52</sup> It is claimed that GSH, ascorbic acid, and metalloproteins are among the biological reducing agents responsible for activation of Pt(IV) prodrugs.<sup>50–53</sup> An important parameter in the mode of action of the Pt(IV) prodrugs is the rate of reduction. As we cannot measure it inside the cancer cells, we compared the rates of reduction of the six new compounds in 50 mM phosphate buffer of pH 7.0 at 37  $^{\circ}\text{C}$ . We expressed their rates of reduction in terms of the half-lives ( $t_{1/2}$ ) of the complexes (Table 1).

The slow rates of reduction observed for compounds **2** ( $t_{1/2} = 35.9$  h) and **3** ( $t_{1/2} = 151.9$  h) are in agreement with the previous reports that Pt(IV) compounds whose coordination sphere is comprised of am(m)ines and carboxylates are reduced slowly, presumably due to the slow transfer of electrons from the ascorbate to the metal.<sup>54</sup> The more rapid

reductions of **1** ( $t_{1/2} = 0.4$  h) and **5** ( $t_{1/2} = 0.5$  h) are attributed to the facile electron transfer from the ascorbate to the metal via an inner-sphere interaction of the ascorbate with the axial hydroxido ligand. Although **4** and **6**, like **2** and **3**, have only am(m)ines and carboxylates in their coordination sphere, they are reduced much more quickly (Table 1). The reason behind this is the relative instability of the DCA ligand to aquation, particularly when both axial ligands are DCA (Table 1).<sup>51,55</sup> Following replacement of the DCA with hydroxide, the rate of reduction increases.

**Anticancer Activity in Cell Culture.** The cytotoxicity of the six Pt(IV) derivatives of  $\text{cis-}[\text{Pt}(\text{NH}_3)(\text{CHA})(\text{OAc})_2]$  was measured in eight cancer cell lines of human and murine origin (Table 2).

Replacing the chlorido ligands of satraplatin by acetates (compound **2**) led to a dramatic reduction in the cytotoxicity. While the average  $\text{IC}_{50}$  values of cisplatin and satraplatin are  $\sim 7$  and  $\sim 5$   $\mu\text{M}$ , respectively, for **1** and **2** it was (depending on the tested cell model) between  $\sim 20$  and  $>100$   $\mu\text{M}$ . Thus, compounds **1** and **2** were basically not active in comparison to cisplatin or satraplatin. Introduction of the bioactive ligands in the axial positions (**3–6**) resulted in a significant enhancement of their potency. The average  $\text{IC}_{50}$  values of compounds **3–6** are 0.6, 1.4, 1.1, and 0.4  $\mu\text{M}$ , respectively. It is worth noting that compounds **3**, **5** and **6** have sub-micromolar activities in all cell lines tested (with the exception of the murine colon carcinoma CT-26), which is in good agreement with previously published data on an oxaliplatin derivative of **5**.<sup>56</sup> Overall, it seems that the concentration range of the compound's cytotoxicity does not depend on the nature of the axial ligand.

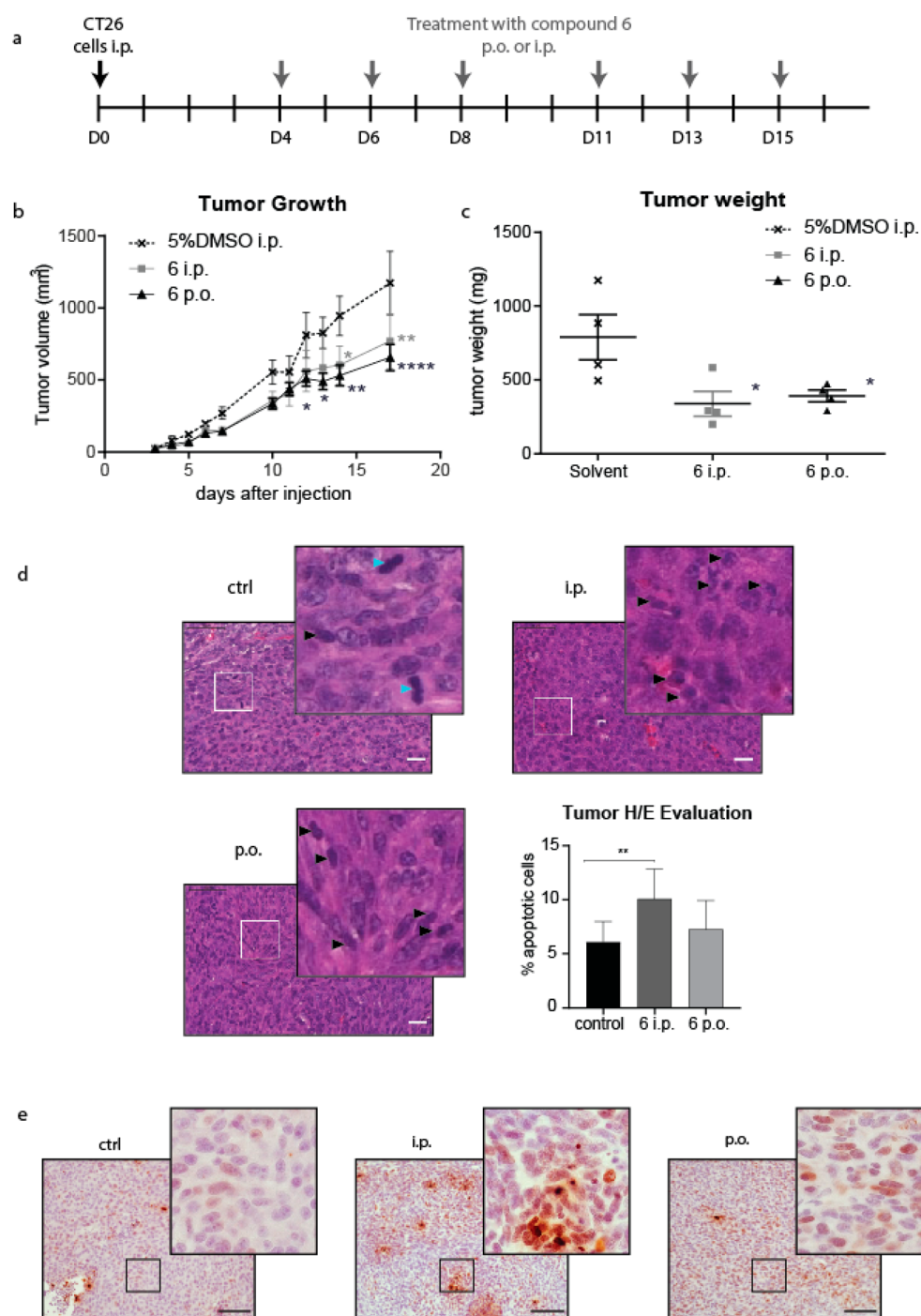


**Figure 6.** In vivo anticancer activity of complex 6. (a) CT-26 cells were injected subcutaneously into the right flank of BALB/c mice. Mice were treated on day 4, 6, 8, 11, 13, and 15 with 20 mg/kg (p.o.) or 7.2 mg/kg (i.p.) of compound 6. (b) Tumor volumes were calculated as described in the [Experimental Section](#). Each experimental group contained four animals. Data are means  $\pm$  SEM. (c) Weight of dissected tumors. (d) Histological evaluation of tumor tissue sections stained by H/E. Blue arrows indicate mitotic cells, and black arrows indicate apoptotic cells: 40 $\times$  magnification, scale bar 25  $\mu$ m, scale bar of bottom corner of enlarged images 50  $\mu$ m. The lower right corner shows quantification of histological sections. Three images of each mouse tumor section were analyzed by manual cell counting of mitotic and apoptotic (pyknotic) cells. Bars depict mean  $\pm$  SD ( $n = 3$ ). Significance was calculated using one-way ANOVA using Graph Pad Prism software. (e) Tumor sections stained for pH2AX: 40 $\times$  magnification, scale bar 50  $\mu$ m, scale bar of bottom corner of enlarged images 50  $\mu$ m.

Consequently, while 4 was slightly less potent than 3, 5, and 6, the last three essentially have similar cytotoxicities. Still, in comparison of the dose–response curves, 6 had the best anticancer activity of all tested drugs in this panel ([Figure S14](#)).

Overall, on the basis of the stability and reduction kinetic data of the compounds ([Table 1](#)), the similarity of the IC<sub>50</sub>

values from 3–6 is rather surprising, which prompted us to further investigate the biological effects of our test panel.

**Cellular Drug Uptake.** In order to better understand the differences in the cytotoxicity of the investigated compounds (especially the lack of activity in case of 1 and 2), the cellular drug uptake levels were investigated by ICP-MS in CT-26 cells.

As shown in Figure 2, distinct differences between the individual compounds were observed. In line with the very high  $IC_{50}$  values obtained in the viability assays, the platinum levels of 1 and 2 were very low (near the limit of detection). This indicates that these compounds have limited anticancer activity due to insufficient drug accumulation. This could be probably explained by a reduced hydrophobicity of these compounds, as indicated by their retention time on a reversed-phase C18 column. Compounds 1 and 2 had retention times of 10.1 and 12.1 min, in comparison those of 5 (with one OH) of 17.9 min and 3, 4, and 6 of >20 min. Interestingly, also compound 5, which was very active in the viability assays, was characterized by a rather low cellular accumulation (below 0.5 ng of Pt/ $10^6$  cells and the reference drug satraplatin). This could probably be explained by the very easy reduction of the compound, resulting in rapid release of the highly active Pt(II) species, enabling earlier DNA damage. Finally, compounds 3, 4, and 6 were very efficiently taken up into the cells (in case of 6 up to 10-fold higher than for satraplatin), which is in good agreement with their anticancer activity in the MTT assays and indicates also that in the case of these compounds the axial ligands facilitate the uptake of these drugs.

**Cell Death, Cell Cycle Arrest, and DNA-Damage-Inducing Properties of the New Complexes.** Despite their similar  $IC_{50}$  values, already rough examination using a cell culture microscope indicated distinct differences in the morphologies of the treated cells. Consequently, the effects of the compound panel were followed by live cell microscopy, which also suggested differences in their underlying mode of actions (e.g., apoptosis-inducing potential; Figure 3a). To gain more insights into the mechanisms of our new platinum drugs, CT26 cells were fixed after 24 h of drug treatment and their DAPI-stained nuclei evaluated for their apoptotic and mitotic features (Figure 3b).

This analysis revealed that only treatment with compounds 3 and 6 led to a significant increase of cells with apoptotic morphology (Figure 3b). Thus, 6 was the most potent apoptosis inducer of the tested cell panel (16-fold increase in comparison to control), while 3 led only to an 8-fold increase in apoptotic cells. No necrotic cells were found in any of the groups (data not shown). With regard to the mitotic fraction, already in the control samples only a very low number of cells with mitotic features was visible (~0.2%). However, a complete absence of mitotic cells in samples treated with compounds 3–6 indicated that all compounds could have an effect on the cell cycle progression of the cancer cells (data not shown). Thus, as a next step, we evaluated the cell cycle distribution in comparison to cisplatin and satraplatin after 24 h of treatment at two concentrations (Figure 4). These experiments revealed that, in line with our hypothesis, 3–6 (1 and 2 were not included because of their inactivity based on insufficient drug uptake) affected the cell cycle distribution of the investigated cancer cells. In more detail, the cells reacted in most cases (especially in the 1  $\mu$ M samples) with a 60–80% increase of the cell population in the G2/M phase (cisplatin was the most potent compound in this aspect, with a significant increase of 240% of the G2/M fraction). In addition, in case of cisplatin, a 3, 4 and 6 shift in the G0/G1-S ratio was observed, which indicated accumulation of cells in the S phase as well as G2/M phase after treatment with these drugs. Whether these differences on cell cycle distribution between 5 and the other compounds could be due to the earlier released PhB ligand is speculative and would

need further investigations. Together these data indicate that, although compounds 3–6 affect the cell cycle progression of the cancer cells, only 3 and 6 are able to induce apoptosis under the investigated conditions.

In order to assess whether the observed effects are due to the more potent formation of DNA adducts, phosphorylation of histone variant H2AX, a common marker for platinum-induced DNA damage,<sup>57,58</sup> was assessed for all drugs. As shown in Figure 5, only compounds 3, 4, and 6 together with cisplatin (which was used as a positive control) were able to significantly increase the signal in comparison to the control samples. Out of these drugs, 6 was most active, resulting in an ~3-fold increase of pH2AX levels in comparison to the control samples. Overall, this indicates that, after 19 h of treatment, at least in the case of 4–6, the Pt(IV) complex was reduced to the active Pt(II) species, which could then bind/interact with the DNA.

**In Vivo Anticancer Activity of Complex 6 against CT26 Colon Cancer Cells in Vivo.** To investigate the anticancer activity of the most promising compound 6 in vivo, female BALB/c mice were injected subcutaneously with CT26 cells into the right flank (day 0), resulting in rapid tumor formation. This model was chosen because it is intrinsically resistant to satraplatin and is only slightly responsive to cisplatin treatment.<sup>59,60</sup> Treatment with 6 was started on day 4 using 7.2 mg/kg i.p. (equimolar to 3 mg/kg for cisplatin and 5 mg/kg for satraplatin) or 20 mg/kg p.o. (a concentration that would be equimolar to 8 mg/kg for cisplatin or 13.5 mg/kg for satraplatin) (Figure 6a). Mice received three therapies per week for 2 weeks. Therapy was well tolerated with no signs of toxicity such as weight loss (data not shown). Although during the first week there were only minor differences in tumor volume between the treatment groups, on day 7 therapy with 6 resulted in tumor stabilization and subsequently slower tumor progression in comparison to the solvent-treated animals. Treatment p.o. via oral gavage had a slightly enhanced anticancer effect in comparison to i.p. application, resulting in significantly reduced tumor volumes (in comparison to control) from day 15 (Figure 6b). On day 18, mice were sacrificed and tumor weights collected. Both treatment groups showed a significant reduction in average tumor weight (over 50%) (Figure 6c). Tumors were subsequently histologically analyzed by H/E staining (for total morphology) and immunohistologically analyzed for occurrence of pH2AX. Morphological analysis of the H/E stains for cells with mitotic and apoptotic features revealed that, while no changes in the levels of mitotic cells were observed (data not shown), in samples collected from mice receiving 6 i.p. significantly enhanced apoptosis levels were detected (Figure 6d). This was associated with higher levels of H2AX phosphorylation (Figure 6e). Overall, this activity of 6 against CT26 cells in vivo is promising, as we have recently shown that this model is intrinsically resistant to satraplatin.<sup>60</sup>

## CONCLUSIONS

In the present paper, we chemically and biologically investigated for the first time the acetato analogues of platinum(IV) derivatives of *cis*-[Pt(NH<sub>3</sub>)(CHA)Cl<sub>2</sub>] with bioactive axial ligands. Replacement of the chlorides with acetates enhanced the water solubility of the compounds. With the exception of the bis-DCA compound 4 all of the compounds were very stable in buffer. Overall, the panel of compounds showed different and partially unexpected

behaviors. On the basis of our previous experience, we expected the rather fast reduction of compounds **1**, **4**, and **5** because of the axial OH ligands of **1** and **5** and the reported fast hydrolysis of one DCA ligand in the cisplatin analogue of **4**. In contrast, the considerably long half-life of **6** (in comparison to **4**) was surprising and indicated that this compound might be attractive for further biological investigations. While replacing the chlorides with acetates in satraplatin led to a reduction in cytotoxicity, the dual- and triple-action analogues with equatorial acetates had low- to sub-micromolar IC<sub>50</sub> values in a panel of eight cancer cell lines. We found that compound **6** was most active in cell culture on the basis of DNA-damage-induced cell cycle inhibition and apoptosis induction. Due to the strong differences in the physicochemical properties, the current compound panel was considered as inappropriate for further biological investigations regarding the role of DCA and PhB ligands in the observed biological activity. However, in case of the triple-action derivative **6**, this definitively needs to be done as a next step in the preclinical evaluation and is a matter of currently ongoing studies. Fortunately, the good activity of compound **6** against CT26 cells in vitro translated into good in vivo efficacy against the CT26 allograft, an in vivo model with intrinsic satraplatin resistance. This indicates that multi-action Pt(IV) derivatives of diamine dicarboxylates are interesting anticancer drug candidates.

## ■ ASSOCIATED CONTENT

### Supporting Information

The Supporting Information is available free of charge at <https://pubs.acs.org/doi/10.1021/acs.inorgchem.9b02796>.

Synthetic protocols, spectroscopic and chromatographic characterization, reduction kinetics, and biological data (PDF)

## ■ AUTHOR INFORMATION

### Corresponding Authors

\*P.H.: tel, +43-1-40160-57594; fax, +43-1-40160-957555; e-mail, [petra.heffeter@meduniwien.ac.at](mailto:petra.heffeter@meduniwien.ac.at).

\*D.G.: tel, +97226758702; e-mail, [dang@ekmd.huji.ac.il](mailto:dang@ekmd.huji.ac.il).

### ORCID

Subhendu Karmakar: 0000-0002-4840-3015

Christian R. Kowol: 0000-0002-8311-1632

Dan Gibson: 0000-0002-1631-4018

### Author Contributions

<sup>||</sup>S.K. and I.P. contributed equally to the main findings of this article

### Notes

The authors declare no competing financial interest.

## ■ ACKNOWLEDGMENTS

D.G. acknowledges the support of the Israel Science Foundation (grant 1002/18) and the Alex Grass Center for Drug Design and synthesis. S.K. wants to thank the Planning and Budgeting Committee (PBC) of the Council for Higher Education (Israel) and The Hebrew University of Jerusalem for a postdoctoral fellowship. We want to acknowledge Dr. Gourab Dey of Prof. Galia Blum's research group for helping with MS measurements. We thank Gerhard Zeitler for devoted animal care, Martin Schaiër for ICP-MS measurements, and Hugo Aborghetti as well as Irene Herbacek for their assistance

with flow cytometry. The study was performed in the course of the COST action CM1105.

## ■ REFERENCES

- (1) Rosenberg, B.; Van Camp, L.; Krigas, T. Inhibition of cell division in *Escherichia coli* by electrolysis products from a platinum electrode. *Nature* **1965**, *205* (4972), 698–9.
- (2) Rosenberg, B.; VanCamp, L.; Trosko, J. E.; Mansour, V. H. Platinum compounds: a new class of potent antitumor agents. *Nature* **1969**, *222* (5191), 385–6.
- (3) Rosenberg, B.; VanCamp, L. Successful regression of large solid sarcoma 180 tumors by platinum compounds. *Cancer Res.* **1970**, *30* (6), 1799–802.
- (4) Kelland, L. The resurgence of platinum-based cancer chemotherapy. *Nat. Rev. Cancer* **2007**, *7* (8), 573–584.
- (5) Wheate, N. J.; Walker, S.; Craig, G. E.; Oun, R. The status of platinum anticancer drugs in the clinic and in clinical trials. *Dalton Trans.* **2010**, *39* (35), 8113–8127.
- (6) Harper, B. W.; Krause-Heuer, A. M.; Grant, M. P.; Manohar, M.; Garbutcheon-Singh, K. B.; Aldrich-Wright, J. R. Advances in Platinum Chemotherapeutics. *Chem. - Eur. J.* **2010**, *16* (24), 7064–7077.
- (7) Johnstone, T. C.; Suntharalingam, K.; Lippard, S. J. The Next Generation of Platinum Drugs: Targeted Pt(II) Agents, Nanoparticle Delivery, and Pt(IV) Prodrugs. *Chem. Rev.* **2016**, *116* (5), 3436–3486.
- (8) Van Den Berg, J. H.; Beijnen, J. H.; Balm, A. J. M.; Schellens, J. H. M. Future opportunities in preventing cisplatin induced ototoxicity. *Cancer Treat. Rev.* **2006**, *32* (5), 390–397.
- (9) O'Dwyer, P. J.; Stevenson, J. P.; Johnson, S. W. Clinical pharmacokinetics and administration of established platinum drugs. *Drugs* **2000**, *59* (Suppl. 4), 19–27.
- (10) McWhinney, S. R.; Goldberg, R. M.; McLeod, H. L. Platinum neurotoxicity pharmacogenetics. *Mol. Cancer Ther.* **2009**, *8* (1), 10–16.
- (11) Kelland, L. R. Preclinical perspectives on platinum resistance. *Drugs* **2000**, *59* (Suppl. 4), 1–8.
- (12) Heffeter, P.; Jungwirth, U.; Jakupec, M.; Hartinger, C.; Galanski, M.; Elbling, L.; Micksche, M.; Keppler, B.; Berger, W. Resistance against novel anticancer metal compounds: Differences and similarities. *Drug Resist. Updates* **2008**, *11* (1–2), 1–16.
- (13) Koeberle, B.; Tomcic, M. T.; Usanova, S.; Kaina, B. Cisplatin resistance: Preclinical findings and clinical implications. *Biochim. Biophys. Acta, Rev. Cancer* **2010**, *1806* (2), 172–182.
- (14) Galluzzi, L.; Senovilla, L.; Vitale, I.; Michels, J.; Martins, I.; Kepp, O.; Castedo, M.; Kroemer, G. Molecular mechanisms of cisplatin resistance. *Oncogene* **2012**, *31* (15), 1869–1883.
- (15) Hall, M. D.; Okabe, M.; Shen, D.-W.; Liang, X.-J.; Gottesman, M. M. The role of cellular accumulation in determining sensitivity to platinum-based chemotherapy. *Annu. Rev. Pharmacol. Toxicol.* **2008**, *48*, 495–535.
- (16) Ang, W. H.; Khalaila, I.; Allardyce, C. S.; Juillerat-Jeanneret, L.; Dyson, P. J. Rational Design of Platinum(IV) Compounds to Overcome Glutathione-S-Transferase Mediated Drug Resistance. *J. Am. Chem. Soc.* **2005**, *127* (5), 1382–1383.
- (17) Hall, M. D.; Mellor, H. R.; Callaghan, R.; Hambley, T. W. Basis for Design and Development of Platinum(IV) Anticancer Complexes. *J. Med. Chem.* **2007**, *50* (15), 3403–3411.
- (18) Johnstone, T. C.; Lippard, S. J. Improvements in the synthesis and understanding of the iodo-bridged intermediate en route to the Pt(IV) prodrug satraplatin. *Inorg. Chim. Acta* **2015**, *424*, 254–259.
- (19) Fokkema, E.; Groen, H. J. M.; Bauer, J.; Uges, D. R. A.; Weil, C.; Smith, I. E. Phase II study of oral platinum drug JM216 as first-line treatment in patients with small-cell lung cancer. *J. Clin. Oncol.* **1999**, *17* (12), 3822–3827.
- (20) Latif, T.; Wood, L.; Connell, C.; Smith, D. C.; Vaughn, D.; Lebwohl, D.; Peereboom, D. Phase II study of oral bis (aceto) ammine dichloro (cyclohexamine) platinum (IV) (JM-216, BMS-182751) given daily x 5 in hormone refractory prostate cancer (HRPC). *Invest. New Drugs* **2005**, *23* (1), 79–84.

- (21) Sternberg, C. N.; Whelan, P.; Hetherington, J.; Paluchowska, B.; Slee, P. H. T. J.; Vekemans, K.; Van Erps, P.; Theodore, C.; Koriakine, O.; Oliver, T.; Lebowitz, D.; Debois, M.; Zurlo, A.; Collette, L. Phase III Trial of Satraplatin, an Oral Platinum plus Prednisone vs. Prednisone alone in Patients with Hormone-Refractory Prostate Cancer. *Oncology* **2005**, *68* (1), 2–9.
- (22) Choy, H. Satraplatin: an orally available platinum analog for the treatment of cancer. *Expert Rev. Anticancer Ther.* **2006**, *6* (7), 973–982.
- (23) Doshi, G.; Sonpavde, G.; Sternberg, C. N. Clinical and pharmacokinetic evaluation of satraplatin. *Expert Opin. Drug Metab. Toxicol.* **2012**, *8* (1), 103–111.
- (24) Gabano, E.; Ravera, M.; Osella, D. Pros and cons of bifunctional platinum(IV) antitumor prodrugs: two are (not always) better than one. *Dalton Trans.* **2014**, *43* (26), 9813–9820.
- (25) Kenny, R. G.; Chuah, S. W.; Crawford, A.; Marmion, C. J. Platinum(IV) Prodrugs - A Step Closer to Ehrlich's Vision? *Eur. J. Inorg. Chem.* **2017**, *2017* (12), 1596–1612.
- (26) Raveendran, R.; Braude, J. P.; Wexselblatt, E.; Novohradsky, V.; Stuchlikova, O.; Brabec, V.; Gandin, V.; Gibson, D. Pt(IV) derivatives of cisplatin and oxaliplatin with phenylbutyrate axial ligands are potent cytotoxic agents that act by several mechanisms of action. *Chem. Sci.* **2016**, *7* (3), 2381–2391.
- (27) Petruzzella, E.; Sirota, R.; Solazzo, L.; Gandin, V.; Gibson, D. Triple action Pt(IV) derivatives of cisplatin: a new class of potent anticancer agents that overcome resistance. *Chem. Sci.* **2018**, *9* (18), 4299–4307.
- (28) Ravera, M.; Gabano, E.; McGlinchey, M. J.; Osella, D. A view on multi-action Pt(IV) antitumor prodrugs. *Inorg. Chim. Acta* **2019**, *492*, 32–47.
- (29) Petruzzella, E.; Braude, J. P.; Aldrich-Wright, J. R.; Gandin, V.; Gibson, D. A Quadruple-Action Platinum(IV) Prodrug with Anticancer Activity Against KRAS Mutated Cancer Cell Lines. *Angew. Chem., Int. Ed.* **2017**, *56* (38), 11539–11544.
- (30) Muhammad, N.; Sadia, N.; Zhu, C.; Luo, C.; Guo, Z.; Wang, X. Biotin-tagged platinum(IV) complexes as targeted cytostatic agents against breast cancer cells. *Chem. Commun.* **2017**, *53* (72), 9971–9974.
- (31) Novohradsky, V.; Zerzankova, L.; Stepankova, J.; Vrana, O.; Raveendran, R.; Gibson, D.; Kasparkova, J.; Brabec, V. Antitumor platinum(IV) derivatives of oxaliplatin with axial valproate ligands. *J. Inorg. Biochem.* **2014**, *140*, 72–79.
- (32) Pathak, R. K.; Wen, R.; Kolishetti, N.; Dhar, S. A Prodrug of Two Approved Drugs, Cisplatin and Chlorambucil, for Chemo War Against Cancer. *Mol. Cancer Ther.* **2017**, *16* (4), 625–636.
- (33) Villar-Garea, A.; Esteller, M. Histone deacetylase inhibitors: Understanding a new wave of anticancer agents. *Int. J. Cancer* **2004**, *112* (2), 171–178.
- (34) Dokmanovic, M.; Clarke, C.; Marks, P. A. Histone Deacetylase Inhibitors: Overview and Perspectives. *Mol. Cancer Res.* **2007**, *5* (10), 981–989.
- (35) Ceccacci, E.; Minucci, S. Inhibition of histone deacetylases in cancer therapy: lessons from leukaemia. *Br. J. Cancer* **2016**, *114* (6), 605–611.
- (36) Mann, B. S.; Johnson, J. R.; Cohen, M. H.; Justice, R.; Pazdur, R. FDA approval summary: vorinostat for treatment of advanced primary cutaneous T-cell lymphoma. *Oncologist* **2007**, *12* (10), 1247–1252.
- (37) Lee, H.-Z.; Kwitkowski, V. E.; Del Valle, P. L.; Ricci, M. S.; Saber, H.; Habtemariam, B. A.; Bullock, J.; Bloomquist, E.; Shen, Y. L.; Chen, X.-H.; Brown, J.; Mehrotra, N.; Dorff, S.; Charlab, R.; Kane, R. C.; Kaminskas, E.; Justice, R.; Farrell, A. T.; Pazdur, R. FDA Approval: Belinostat for the Treatment of Patients with Relapsed or Refractory Peripheral T-cell Lymphoma. *Clin. Cancer Res.* **2015**, *21* (12), 2666–2670.
- (38) Barbarotta, L.; Hurley, K. Romidepsin for the Treatment of Peripheral T-Cell Lymphoma. *J. Adv. Pract. Oncol.* **2015**, *6* (1), 22–36.
- (39) Raedler Lisa, A. Farydak (Panobinostat): First HDAC Inhibitor Approved for Patients with Relapsed Multiple Myeloma. *Am. Health Drug Benefits* **2016**, *9* (Spec Feature), 84–7.
- (40) Yee, A. J.; Raje, N. S. Panobinostat and Multiple Myeloma in 2018. *Oncologist* **2018**, *23* (5), 516–517.
- (41) Michelakis, E. D.; Webster, L.; Mackey, J. R. Dichloroacetate (DCA) as a potential metabolic-targeting therapy for cancer. *Br. J. Cancer* **2008**, *99* (7), 989–994.
- (42) Bonnet, S.; Archer, S. L.; Allalunis-Turner, J.; Haromy, A.; Beaulieu, C.; Thompson, R.; Lee, C. T.; Lopaschuk, G. D.; Puttagunta, L.; Bonnet, S.; Harry, G.; Hashimoto, K.; Porter, C. J.; Andrade, M. A.; Thebaud, B.; Michelakis, E. D. A mitochondria-K<sup>+</sup> channel axis is suppressed in cancer and its normalization promotes apoptosis and inhibits cancer growth. *Cancer Cell* **2007**, *11* (1), 37–51.
- (43) Cairns, R. A.; Papandreou, L.; Sutphin, P. D.; Denko, N. C. Metabolic targeting of hypoxia and HIF1 in solid tumors can enhance cytotoxic chemotherapy. *Proc. Natl. Acad. Sci. U. S. A.* **2007**, *104* (22), 9445–9450.
- (44) Pearson, H. Cancer patients opt for unapproved drug. *Nature* **2007**, *446* (7135), 474–475.
- (45) Wong, J. Y. Y.; Huggins, G. S.; Debidda, M.; Munshi, N. C.; De Vivo, I. Dichloroacetate induces apoptosis in endometrial cancer cells. *Gynecol. Oncol.* **2008**, *109* (3), 394–402.
- (46) Hoefler, D.; Varbanov, H. P.; Legin, A.; Jakupec, M. A.; Roller, A.; Galanski, M.; Keppler, B. K. Tetracarboxylatoplatinum(IV) complexes featuring monodentate leaving groups - A rational approach toward exploiting the platinum(IV) prodrug strategy. *J. Inorg. Biochem.* **2015**, *153*, 259–271.
- (47) Egger, A.; Rappel, C.; Jakupec, M. A.; Hartinger, C. G.; Heffeter, P.; Keppler, B. K. Development of an experimental protocol for uptake studies of metal compounds in adherent tumor cells. *J. Anal. At. Spectrom.* **2009**, *24*, 51–61.
- (48) Zhang, J. Z.; Bonnitcha, P.; Wexselblatt, E.; Klein, A. V.; Najajreh, Y.; Gibson, D.; Hambley, T. W. Facile Preparation of Mono-, Di- and Mixed-Carboxylato Platinum(IV) Complexes for Versatile Anticancer Prodrug Design. *Chem. - Eur. J.* **2013**, *19* (5), 1672–1676.
- (49) Wexselblatt, E.; Yavin, E.; Gibson, D. Platinum(IV) Prodrugs with Haloacetato Ligands in the Axial Positions can Undergo Hydrolysis under Biologically Relevant Conditions. *Angew. Chem., Int. Ed.* **2013**, *52* (23), 6059–6062.
- (50) Hall, M. D.; Hambley, T. W. Platinum(IV) antitumor compounds: their bioinorganic chemistry. *Coord. Chem. Rev.* **2002**, *232* (1–2), 49–67.
- (51) Wexselblatt, E.; Gibson, D. What do we know about the reduction of Pt(IV) pro-drugs? *J. Inorg. Biochem.* **2012**, *117*, 220–229.
- (52) Gibson, D. Platinum(IV) anticancer prodrugs - hypotheses and facts. *Dalton Trans.* **2016**, *45* (33), 12983–12991.
- (53) Novakova, O.; Vrana, O.; Kiseleva, V. I.; Brabec, V. DNA interactions of antitumor platinum(IV) complexes. *Eur. J. Biochem.* **1995**, *228* (3), 616–24.
- (54) Zhang, J. Z.; Wexselblatt, E.; Hambley, T. W.; Gibson, D. Pt(IV) analogs of oxaliplatin that do not follow the expected correlation between electrochemical reduction potential and rate of reduction by ascorbate. *Chem. Commun.* **2012**, *48* (6), 847–849.
- (55) Wexselblatt, E.; Raveendran, R.; Salameh, S.; Friedman-Ezra, A.; Yavin, E.; Gibson, D. On the stability of Pt(IV) pro-drugs with haloacetato ligands in the axial positions. *Chem. - Eur. J.* **2015**, *21* (7), 3108–3114.
- (56) Zajac, J.; Kostrhunova, H.; Novohradsky, V.; Vrana, O.; Raveendran, R.; Gibson, D.; Kasparkova, J.; Brabec, V. Potentiation of mitochondrial dysfunction in tumor cells by conjugates of metabolic modulator dichloroacetate with a Pt(IV) derivative of oxaliplatin. *J. Inorg. Biochem.* **2016**, *156*, 89–97.
- (57) Gomes, L. R.; Rocha, C. R. R.; Martins, D. J.; Fiore, A.; Kinker, G. S.; Bruni-Cardoso, A.; Menck, C. F. M. ATR mediates cisplatin resistance in 3D-cultured breast cancer cells via translesion DNA synthesis modulation. *Cell Death Dis.* **2019**, *10* (6), 459.

(58) Adam-Zahir, S.; Plowman, P. N.; Bourton, E. C.; Sharif, F.; Parris, C. N. Increased gamma-H2AX and Rad51 DNA Repair Biomarker Expression in Human Cell Lines Resistant to the Chemotherapeutic Agents Nitrogen Mustard and Cisplatin. *Chemotherapy* **2014**, *60* (5–6), 310–20.

(59) Theiner, S.; Varbanov, H. P.; Galanski, M.; Egger, A. E.; Berger, W.; Heffeter, P.; Keppler, B. K. Comparative in vitro and in vivo pharmacological investigation of platinum(IV) complexes as novel anticancer drug candidates for oral application. *J. Biol. Inorg. Chem.* **2015**, *20* (1), 89–99.

(60) Mayr, J.; Heffeter, P.; Groza, D.; Galvez, L.; Koellensperger, G.; Roller, A.; Alte, B.; Haider, M.; Berger, W.; Kowol, C. R.; Keppler, B. K. An albumin-based tumor-targeted oxaliplatinprodrug with distinctly improved anticancer activity in vivo. *Chem. Sci.* **2017**, *8* (3), 2241–2250.